Bending Dynamics and Directionality Reversal in Liquid Crystal Network Photoactuators

Casper L. van Oosten,*,† Daniel Corbett,‡ Dylan Davies,† Mark Warner,‡ Cees W. M. Bastiaansen,† and Dirk J. Broer†,§

Eindhoven University of Technology, Post Office Box 513, NL-5600 MB Eindhoven, The Netherlands, Cavendish Laboratory, Madingley Road, Cambridge, CB3 0HE, United Kingdom, and Philips Research Laboratories, High Tech Campus 4, NL-5656AE Eindhoven, The Netherlands

Received August 7, 2008; Revised Manuscript Received September 11, 2008

ABSTRACT: Liquid crystalline photoactuators typically bend toward the light source, driven by the isomerization of azobenzene. In samples with a relatively large thickness and high azobenzene loading such as LC photoactuators, intense optical beams are seen to be absorbed in spatially nonexponential ways. Here we show that the dynamics of the related mechanical behavior is also strongly nonlinear, where the actuator reaches a maximum bend before unbending again to its equilibrium deformed state. The effect is amplified when combined with actuators with an internal composition gradient, leading to a reversal of the bending direction away from the light source.

Introduction

The dynamics of the *trans*−*cis* isomerization of azobenzene in a polymer network has attracted attention for both fundamental studies of polymer behavior and practical applications. The isomerization causes a change in the absorbance spectrum of the azobenzene unit, and through the dynamics of this optical change, the azobenzene unit is able to report on the local rigidity of its surroundings.[1,2] In an ordered liquid crystalline network, the *trans*−*cis* isomerization of azobenzene leads to an order reduction, causing a macroscopic contraction along the molecular director and an expansion perpendicular to it.[3] In this way, the polymer functions as a photomechanical actuator. The classical case of the liquid crystal network or liquid crystal elastomer based photoactuator is that of a film with a planar uniaxial molecular director, where the gradient in light intensity through the thickness of the film causes bending.[4−10] Recently we showed that the transmission of light through these actuators follows a nonexponential behavior in time, strongly deviating from those cases where the absorption is low.[11] In these high-absorbing actuators, the isomerization gradient forms the basis of the photomechanical response and drives the directionality of the shape deformation. It is the dynamics and directionality of this shape deformation that is the focus of this work. Here, we shall first use a theoretical approach to describe the dynamics of the photo bending. We start with the dynamics of the optical response, which will be expanded to predict the mechanical behavior. Two cases will be considered: the classic case of the LC photoactuator with planar uniaxial molecular director and a new type of photoactuator with internal composition gradient. In both cases, we will observe a complex, nonexponential behavior in time. Using experiments, we will show that this theory matches the experiments. In the last part of this work, we will show that the systems with the internal composition gradient show a reversal in bending direction upon prolonged exposure.

Under normal room conditions, azobenzene dyes are mostly in their elongated *trans*-state. A typical azobenzene molecule is A3MA, as shown in Figure 1, which has an absorption maximum in the UV at 356 nm. Upon exposure to UV light, the molecule undergoes an isomerization to the bent *cis*-state. The sample changes color as the absorption of UV light decreases and the absorption of visible light increases. For A3MA, the *cis*-state has absorption peaks in the visible at about 450 nm and in the near UV at about 310 nm, with a significant reduction of the absorption at 356 nm (Figure 1b). Relaxation back to the *trans*-state is driven thermally and by exposure to light at the peak wavelengths of the *cis*-state. The photostationary, UV-illuminated state is therefore an equilibrium state between the forward *trans*−*cis* isomerization rate and the thermal relaxation rate.

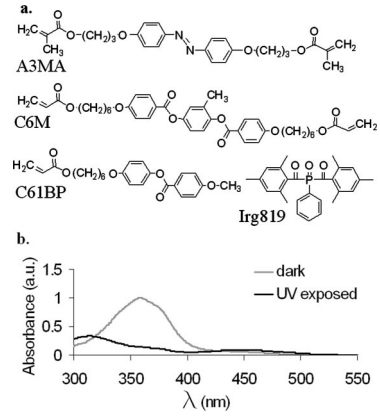

Figure 1. Molecular structures (a) and absorption spectra of A3MA for the dark (*trans*-dominated) and UV-exposed (*cis*-dominated) states (b).

One convenient way to optically characterize a film is by its ratio of the Beer absorption length of the *trans*-state d_t to the film thickness w.[12] The Beer absorption length is a measure for the absorptivity of the material and depends on material parameters such as dye concentration. For films with moderate to high dye loads ($w/d_t > 1$), the transmission of intense beams of light through the film follows a nonexponential profile both in space and time.[11,13] We will first adopt the analysis of the dynamics of the optical absorption from previous work[11] and then introduce the analysis of the effected mechanical behavior. Assuming the back relaxation only happens thermally, the dynamics of the isomerization can be written as

* To whom correspondence should be addressed. E-mail: c.l.v.oosten@tue.nl.
† Eindhoven University of Technology.
‡ Cavendish Laboratory.
§ Philips Research Laboratories.

10.1021/ma801802d CCC: $40.75
Published on Web 10/23/2008

$$\partial n_t/\partial t = -\Gamma I n_t + n_c/\tau \quad (1)$$

where n_t is the number fraction of *trans*-azobenzene, $n_c = 1 - n_t$ the number fraction of *cis*-azobenzene, Γ determines the rate of $t \rightarrow c$ transition, τ is the rate of thermal back relaxation, and I the intensity of the light. Here, we make the simplification that Γ is independent of the nematic order, that is, the absorption of the *trans*-chromophores does not change with the order parameter. To characterize the intensity of the beam in relation to the material, we define the material by the intensity $I_t = 1/(\Gamma\tau)$ and find a measure for the incident beam using $\alpha = I_0/I_t$, where I_0 is the incident intensity of the light. When a LC film containing azobenzene units and with $w \gg d_t$ is exposed to UV light, initially only the top layer of the film isomerizes due to the high absorption. As absorption decreases in this top layer, more light is transmitted through the films, and the layers below are bleached. In effect, this behavior can be described as a "front of bleaching" moving through the film from the top to the bottom. If we define the local relative intensity $|(x,t) = I(x,t)/I_0$ and assume no optically stimulated back reaction, this bleaching is visualized in an increase in the number density of *cis*-azobenzene n_c in space and time

$$n_c(x,t) = 1 + d_t\frac{\partial}{\partial x}\ln(|) \quad (2)$$

Figure 2 shows this propagation of the region with a high *cis*-concentration through the sample. When the bleaching effect is large enough, that is, $\Gamma I > 1/\tau$, there is almost no gradient in *cis*-nematogens n_c left in the film in the photostationary illuminated state. The gradients at $t/\tau = 5$ in Figure 2 are close to the steady gradients, showing little bleaching for $\alpha = 2$ and high bleaching for $\alpha = 10$. Experimentally, it is often more convenient to measure the relative intensity of the light transmitted through the film, which can be calculated by inverting

$$t/\tau = \int_{x/d}^{A} \frac{dA}{x/d - \alpha - A + \alpha e^{-A}} \quad (3)$$

wherein $A(x,t) = -\ln(|)$.[11] The quantity A looks very much like the standard absorbance, but in nonexponential cases, it will depend in a complex way on depth x.

Now, we make the connection to the macroscopic mechanical deformation of the material. The equilibrium deformation of the beam is found by balancing the photoinduced strains ε_{photo} in the plane of the film with the bending and in-plane strains.[14] The resultant strain, ξ, relative to the photostrain at each depth x, is given by

$$\xi(x,t) = \frac{x}{R} + K - \varepsilon_{photo}(x,t) \quad (4)$$

where x denotes the location in thickness, K denotes a uniform in-plane contraction, and t denotes the time. The bending radius

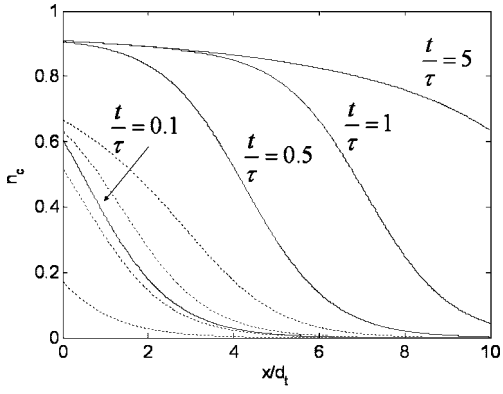

Figure 2. Profiles of number fraction *cis*-azobenzene n_c propagating through the thickness x of the sample at times $t/\tau = 0.1$, 0.5, 1.5, and 5 and for $\alpha = 2$ (dashed lines) and $\alpha = 10$ (solid lines).

R as a function of thickness w and photostrains ε_{photo} can be found by applying the conditions of zero-net force and zero-net moment, arising from the elasting effect of the net strain ξ. These conditions result in

$$\frac{1}{R} = \frac{12}{w^3}\int_0^w \left(x - \frac{w}{2}\right)\varepsilon_{photo}dx \quad (5)$$

It has been shown[15] that for the low end of the azo-concentrations (up to 10 wt %), the photoinduced deformation scales simply with the concentration of *cis*-azobenzene and thus

$$\varepsilon_{photo}(x,t) = P(x)n_c(x,t) \quad (6)$$

where $P(x)$ is the photoresponsivity of the material. The magnitude of P depends on a number of parameters such as the initial order of the system, the molecular director orientation, the cross-link density of the network, and the temperature relative to the glass-transition temperature of the network. Here we work with a glassy polymer and therefore assume small (<1%) strains and small changes in order parameter, typically from 0.6 to 0.5. As the motions are relatively slow with respect to the dimensions and weight of these systems, we assume that inertia plays no role and the bending dynamics are entirely aslaved to those of absorption.[16] Further on in this work we will introduce actuators with a composition gradient in thickness and, therefore, allow $P(x)$ to be a linear function: $P(x) = a_1 + a_2x$. Substituting this into eq 5, rewriting it, and performing integration by parts results in

$$\frac{1}{R} = 12\left(\frac{d_t}{w}\right)^3\left[-\frac{w}{2d_t}\frac{P(w)}{d_t}\ln|_w - \frac{a_2}{12}\left(\frac{w}{d_t}\right)^3 + \int_0^w \ln|_w\left\{\frac{a_1}{d_t} + a_2\left(2\frac{x}{d_t} - \frac{w}{2d_t}\right)\right\}\frac{dx}{d_t}\right] \quad (7)$$

In the classic case of a homogeneous photoactuator, one can assume that $P(x)$ is constant throughout the thickness: $P(x) = a_1$. Following the evolution of the bending radius in time, d_t/R first increases in time to a maximum before it reaches an equilibrium, less bent state. A sketch of this behavior is shown in Figure 3.

We seek to further exploit the relaxation of the bend and amplify it. To do so, we use the fact that the maximum deformation depends on the local properties of the polymer matrix, expressed in the $P(x)$ in eq 6, that is $a_2 \neq 0$. Polymers with a lower number of cross-links have more rotational freedom for internal molecular reorganization and are therefore able to show larger deformation for the same input, down to a certain lower limit of cross-links. For instance, it was shown[17] that a small reduction of 5 wt % in concentration of diacrylate cross-linkers resulted in a large, 20% increase in contraction. At homogeneous order reduction, an aligned uniaxial planar actuator with lower density of cross-links at the bottom than at the top would thus contract more at the bottom and bend down.

Films with an internal gradient in cross-link density can be made using a mix of mesogenic mono- and diacrylates, an optical absorber and a photoinitiator that are active at the same wavelengths.[18] The absorber causes a gradient in light intensity through the thickness of the sample. During polymerization the diacrylate monomer has a higher probability to be captured and connected to the forming network than the monoacrylate monomer. Therefore, the diacrylate, as a free, nonbound molecule, is depleted faster than the monoacrylate. As the overall polymerization rate scales with the light intensity, this is especially the case at the location of high intensity at the top. This causes a concentration driven diffusion of diacrylate monomer to the top of the film during polymerization (Figure 4). Being a diffusion-limited process, the light intensity during the polymerization offers control over the steepness of the

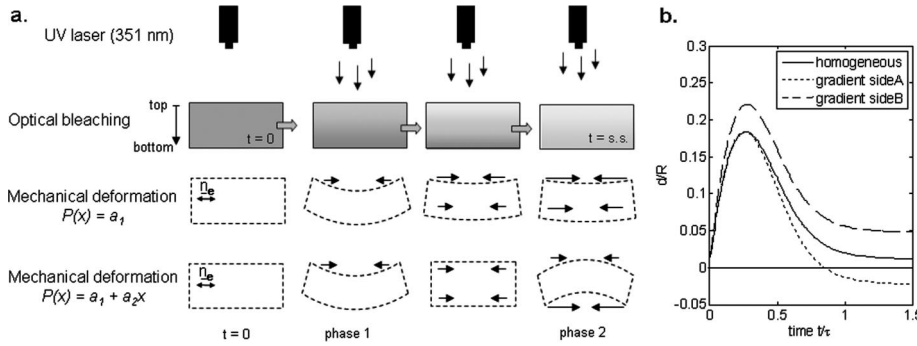

Figure 3. (a) Schematic illustration of the optical bleaching and the mechanical responses of actuators with homogeneous composition and with a concentration gradient, from the initial situation to the illuminated steady state (s.s.). (b) Plot of curvature d/R against time t/τ, with $\alpha = 10$, $w/d = 5$ for a homogeneous sample (solid lines) with $P(x) = -1$, for a sample with internal gradient illuminated from side A (dashed lines), $P(x) = -(1 + 0.2x/w)$ and the same sample illuminated from side B, $P(x) = -(1.2 - 0.2x/w)$.

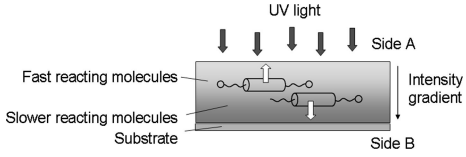

Figure 4. Schematic illustration of the process to create a polymerization induced concentration gradient. Side A of the sample is the side closest to the light source during polymerization and side B is furthest.

gradient: At lower intensities, there is more time for the diffusion to take place, creating a steeper gradient. For convenience, we will call the top side during polymerization side A and the bottom of the sample side B.

For the present system, it suffices to add the monoacrylate C61BP (Figure 1) to produce the gradient in cross-link density. The azobenzene A3MA acts as an absorber for the wavelengths that the photoiniator Irg819 dissociates at, thus creating the desired gradient during polymerization. In this system, an additional complexity arises due to the reactive azobenzene monomers. As they are bifunctional as the C6M, they are expected to diffuse to some extent to the high intensity areas. Moreover, in copolymerization with acrylates, methacrylates usually have a higher reaction rate than acrylates, and thus, diffusion of the dimethacrylate azobenzene to the high intensity region at the top is even enhanced.[19,20] This azobenzene gradient generates an effect opposite to that of the modulus (cross-link density) gradient. Therefore, we choose to optimize the system by making a number of samples under different light intensities for the photopolymerization.

Assessing the bending dynamics of these gradient actuators, when illuminated from side A, two phases can be distinguished. At the beginning, the light gradient through the film is so strong that it dominates and the film bends over side A toward the light. When much of the film is bleached, in the second phase, the lower cross-linked side B allows for more contraction. The gradient in cross-link-density dominates over the gradient in azobenzene concentration and the film bends over side B, away from the light. In this way, a 2-way bending actuator is created using a single continuous input, making the behavior highly nonlinear.

Materials and Methods

Samples were prepared with the azo-dye A3MA and reactive mesogen C6M (Figure 1). A photoinitiator (Ciba Irgacure 819, 1 wt %) was added and the mixture was filled into a homemade glass cell with 20 μm spacing treated with planar-aligning polyimide on the inside. The cell was filled in the isotropic phase at 125 °C, after which it was cooled to the nematic phase and the mixture photopolymerized for 180 s at 92 °C using a high-pass optical filter such that $\lambda > 400$ nm. After the photopolymerization, the samples were heated to 150 °C to ensure complete conversion of the acrylate groups and remove any stress that may have been caused by polymerization shrinkage. Three different polymer films were made with 0.5, 1.5, and 4.0 wt % A3MA.

The dynamics of the optical response of these films was measured in a laser setup using an Ar laser with emission at 351 nm, close to the absorption maximum of the trans-state at 356 nm, during the first 180 s of exposure. The transmitted intensity of the laser-light through the polymer film was measured using a Newport 4832-C Optical Power Meter and recorded at 10 Hz using a PC running LABView. A cell filled with poly(C6M) was used to record a baseline for the measurement; the intensity of the laser light was 150 mW/cm^2, with the polarization state of the light always parallel to the molecular director. Although polarized light is no prerequisite for the effects described here, the azobenzene dye is dichroitic, giving the sample a preferential absorption along the director. Any other polarization state of the light with respect to the film would thus lead to a lower absorption. In that case, the isomerization of azobenzene through the thickness of the film proceeds slower.

After optical characterization, the cells were carefully opened with a razorblade and a strip of 4 mm wide and 10 mm long was cut with the length of the strip parallel to the director. The films were clamped such that about 7 mm was still freestanding and consequently exposed with the same laser light. The motion of the film was recorded using a digital camera at 15 fps. The bending radius was analyzed for a selection of the frames by manually fitting a circle to the movie stills. The fit was made only with the top part of the actuator where the bend was sharpest; the parts of the actuator that received little light due to the bend state were ignored.

For the samples with an internal cross-link gradient, a mix was made with mesogenic mono- and diacrylates in a weight ratio of 2:3. The concentration of A3MA was chosen 4 wt % to allow comparison with the films without a gradient, making the total monomeric composition 55 wt % C6M, 40 wt % C61BP, 4 wt % A3MA, and 1 wt % Irg819. The nematic phase of the mixture was much reduced by the addition of the monoacrylate and, therefore, the curing temperature was set to 40 °C. A band-pass filter (320−370 nm) was used in combination with a UV-lamp (Hg) for the polymerization. The samples were polymerized with light intensities ranging from 0.5 to 10 mW/cm^2. A first check on the gradient in the film was made by heating of the film above a hotplate. These films bend under a homogeneous order reduction to side B. The composition gradient was confirmed by ATR IR-spectrometry measurement, where the composition of the outer surface layers of the film is analyzed within 1 μm from the surface.

The bending behavior of the film was analyzed in the same laser setup while keeping track of the orientation of the higher- and lower cross-linked sides. The radius of curvature was measured, where bending toward the laser light is defined as positive bending.

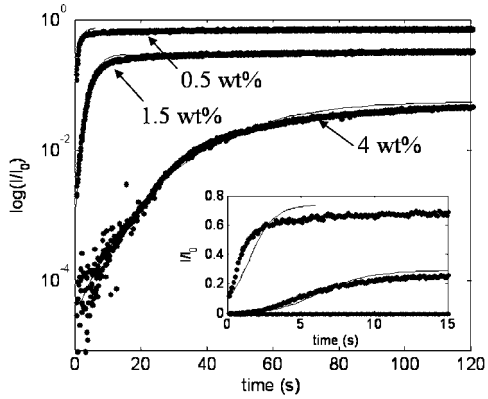

Figure 5. Transmittance of laser light ($\lambda = 351$ nm, $I = 150$ mW/cm^2) through 20 μm samples of poly(C6M/A3MA) with weight concentrations of 0.5, 1.5, and 4 wt % (dots). The solid lines show the fit using $\alpha = 8$, $\tau = 6$ for the samples with 0.5 and 1.5 wt % and $\tau = 30$ for 4.0 wt %. The inset shows a detail of the plot with a linear I/I_0 axis.

Results and Discussion

The nonexponential increase of transmitted light through the samples was found for the samples with 1.5 and 4.0 wt % A3MA but was less pronounced at the sample with the lower dye load of 0.5 wt % (Figure 5). By evaluating the transmission at $t = 0$ and assuming a Beer-like attenuation profile, one can extract the *w/d* ratios for these samples: 2.3, 6.9, and 10.4 for 0.5, 1.5, and 4.0 wt %, respectively. By fitting eq 3 to the transmission profiles, one can obtain the values of α and the time constant τ. A good fit was obtained with $\alpha = 8$ and $\tau = 6$ for the samples with 0.5 and 1.5 wt % and $\tau = 30$ for 4.0 wt %. There is a consistent deviation in the optical properties of the 4 wt % sample. As one would expect, the *w/d* ratios to scale linearly with concentration of azobenzene, the *w/d* value is relatively low for the 4 wt % A3MA sample. This internal inconsistency in the time-scale fit was found upon repetition of the experiment. We speculate that the deviation of the model at higher dye loadings is caused by interactions of the azobenzene with itself.

The mechanical bending of the film was studied for the films with 1.5 and 4.0 wt % of A3MA. Figure 6a shows the main stages of the motion: the films reach a maximum in bending and then slowly relax back to a less bend state, while the UV light was kept on. Here, there is only a gradient in light intensity through the film present. The influence of gravity or heating is limited here: the films showed the same behavior in a standing configuration rather than a hanging configuration. Furthermore, these films are glassy at room temperature with a modulus of around 1.1 GPa parallel to the director and 0.5 GPa perpendicular to it.[6]

Of course, the sample with 4 wt % A3MA is able to show larger deformation as a result of the higher azobenzene content. The bending of this sample is so strong that it eclipses itself after about 6 s. The eclipsing causes part of the sample to receive less light, giving it the opportunity to relax back, while the end part of the strip is now illuminated from the other side, thereby causing this end part to slightly bend in the other direction. Finally, the film is bleached so much that the bend reduces to a final state that is curved only slightly more than the initial position. A plot of the bending radius is given in Figure 6b.

A good fit with the model was found for $\alpha = 6$, $\tau = 2.6$, and $P(x) = -0.865$ mm^{-1} (1.5 wt % sample) and $\alpha = 6$, $\tau = 13$, and $P(x) = -1.73$ mm^{-1} (4 wt % sample). However, the fit parameters differ from the values found in the optical fit: α is slightly lower, 6 instead of 8, but more striking is the reduction of the time scale τ by a factor 2.3. The difference in α may be explained by the fact that the optical measurements were performed on films that were not allowed to bend, and thus, obliquity factors do not play a role there. The difference in timescales is the focus of a current study and we plan to report on this in future work.

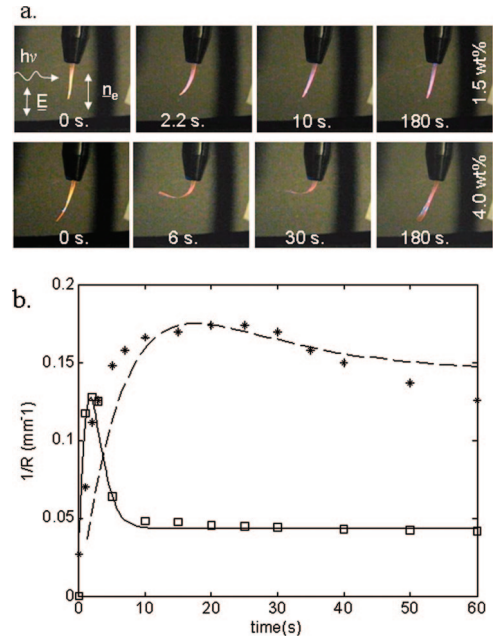

Figure 6. (a) Bending of uniaxial planar aligned films with 1.5 (top) and 4.0 wt % of A3MA upon exposure of laser light (351 nm) from the left side with $I = 150$ mW/cm^2. The propagation direction and polarization state of the light and the molecular orientation of the actuators are sketched on the right. (b) Experimental bending radius (symbols) and modeled bending radius (lines). Fits for the 1.5 wt % sample (□ and solid line) were obtained with $\alpha = 6$, $\tau = 2.6$ s, and $P(x) = -0.865$ mm^{-1}, a fit for the 4 wt % sample (* and dashed line) was obtained using $\alpha = 6$, $\tau = 13$ s, and $P(x) = -1.73$ mm^{-1}.

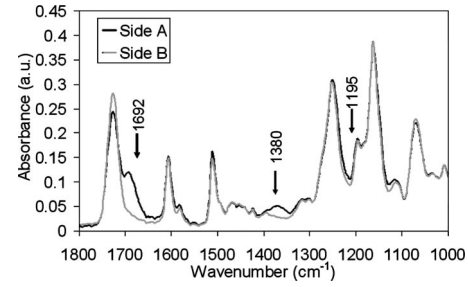

Figure 7. ATR FT-IR spectra of a single film taken from both sides of a film with internal cross-link gradient, polymerized at 10 mW/cm^2.

As a next step, the films with the internal cross-link gradient were evaluated. As expected, the IR data revealed two gradients (Figure 7). The first gradient is in cross-link density, visible from the peaks at 1195 cm^{-1}, ascribed to the O−CH$_3$ group of C61BP and at 1692 cm^{-1}, ascribed to the C═O stretching in the acrylate groups.[21] The measurement of the peak surface indicated a concentration difference of the monoacrylate of 45 wt % at side A and 35 wt % at side B. A second gradient is found in the azobenzene, visible from the broad peak around 1380 cm^{-1}. The azobenzene gradient is estimated to be from 5 wt % on side A and 3 wt % on side B.

The actuators made with photopolymerization intensities of 0.5 mW/cm^2 to 10 mW/cm^2 all showed the reversal of bending direction upon prolonged exposure. A typical response is given in Figure 8. Upon illumination from side A, the films first rapidly bend toward the light source. Upon prolonged exposure, the films relax similar to the films without a gradient, but eventually reach a position curving in the opposite direction. The samples

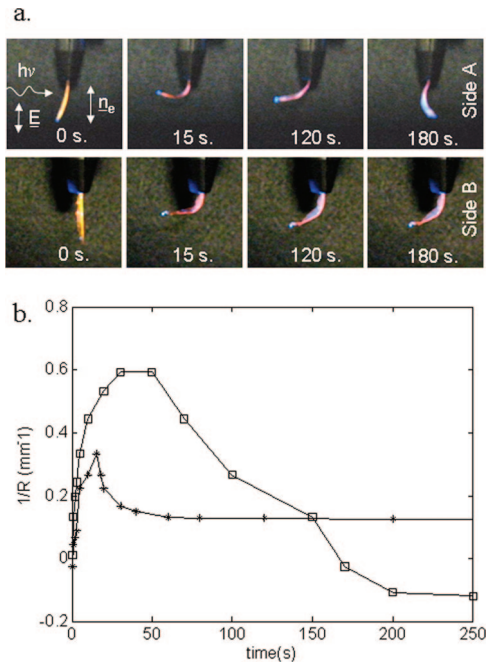

Figure 8. (a) Bending of a planar uniaxially aligned actuator with internal composition gradient of poly(C6M/C61BP/A3MA), polymerized at 10 mW/cm^2 and illuminated with laser light coming from the left of 150 mW/cm^2 at 351 nm. The top sequence shows the response of the film oriented with side A toward the laser light, the bottom sequence shows the same film, but now oriented with side B toward the laser light. The polarization state of the light and the orientation of the nematic director in the samples are denoted with $\underline{E}$ and $\underline{n}_e$ (b) Curvature $1/R$ for the gradient sample cured with 10 mW/cm^2, side A (□) and side B (*).

polymerized at 5 and 10 mW/cm^2 showed a larger backward bend then the samples made with 0.5 and 1 mW/cm^2. One explanation for the poorer performance of the samples polymerized at lower intensities is that there the gradient in azobenzene intensity may start to dominate over the effect of the cross-link gradient. Furthermore, samples polymerized at an intensity of 0.5 mW/cm^2 and 1 mW/cm^2 sometimes twisted over their length axis, showing the presence of two competing bending axes.

The development of the bending radius in time is shown in Figure 8b. The shape of the response was similar for all samples. The typical speeding up of the response when the sample returns to its elongated, unbent state (at 150 s in Figure 8b), was not predicted in our model. When unbending, the sample catches more light and, therefore, the motion speeds up to a maximum, slowing down again when the sample bends away from the light. These obliquity factors were not included in the model. Although the glass-transition temperatures of the films have been lowered compared to the films without internal composition gradient, there is no significant increase in response time, as the films are still glassy at room temperature. The responses of sides A and B are qualitatively similar to the theoretically predicted response in Figure 3b. At this stage, it is not yet possible to obtain a quantitative fit for these gradient systems, as there is too little known on the relation between the chemical composition and the maximum deformations, that is, the exact shape of $P(x)$ for these systems.

The two-directional bending in this system occurs over time scales that are long for practical applications of these systems as actuators in devices. However, this relatively slow system is suitable for demonstrating the nuances of the dynamics, showing that a response is much more complex than a simple exponential curve. Other authors have shown that with slightly different choices of azobenzene guests and LC hosts, very fast systems can be constructed.[5,22] The two-way bending of this system offers a road to more control and added versatility of these optically driven actuators.

Conclusions

The photostimulated bending of light-driven LC actuators driven by the isomerization of azobenzene shows a nonlinear response in time. It was shown that the bending of these actuators reaches a maximum bent state much before the equilibrium deformation is reached. This bending behavior was modeled, showing a good fit with experiments. Actuators with an internal composition gradient can be simply created by using a mixture of mono- and difunctional reactive mesogens. These actuators with composition gradient can be used to amplify the relaxation of the bending, leading to a reversal of the bending direction upon continuous illumination. This two-way bending opens the road to new potential applications for light-driven LC network actuators.

Acknowledgment. We thank Pit Teunissen for the IR measurements. Part of this work was financially supported by the Dutch Polymer Institute under Project No. 532 and part by the EPSRC.

Supporting Information Available: Movie files of the actuators. This material is available free of charge via the Internet at http://pubs.acs.org.

References and Notes

(1) Eisenbach, C. D *Polymer* **1980**, *21*, 1175–1179.
(2) Evans, R. A.; Hanley, T. L.; Skidmore, M. A.; Davis, T. A.; Such, G. K.; Yee, L. H.; Ball, G. E.; Lewis, D. A. *Nat. Mater.* **2005**, *4*, 249–253.
(3) Finkelmann, H.; Nishikawa, E.; Pereira, G. G.; Warner, M. *Phys. Rev. Lett.* **2001**, *87*, 015501.
(4) Yu, Y. L.; Nakano, M.; Ikeda, T. *Nature* **2003**, (425), 145.
(5) Camacho-Lopez, M.; Finkelmann, H.; Palffy-Muhoray, P.; Shelley, M. *Nat. Mater.* **2004**, *3*, 307–310.
(6) Harris, K. D.; Cuypers, R.; Scheibe, P.; Van Oosten, C. L.; Bastiaansen, C. W. M.; Lub, J.; Broer, D. J. *J. Mater. Chem.* **2005**, *15*, 5043–5048.
(7) Tabiryan, N.; Serak, S.; Dai, X. M.; Bunning, T. *Opt. Express* **2005**, *13*, 7442–7448.
(8) Kondo, M.; Yu, Y.; Ikeda, T. *Angew. Chem., Int. Ed.* **2006**, *45*, 1378.
(9) Yamada, M.; Kondo, M.; Mamiya, J.; Yu, Y.; Kinoshita, M.; Barrett, C. J.; Ikeda, T. *Angew. Chem., Int. Ed.* **2008**, *47*, 4986–4988.
(10) Koerner, H.; White, T. J.; Tabiryan, N. V.; Bunning, T. J.; Vaia, R. A. *Mater. Today* **2008**, *11*, 34–42.
(11) Corbett, D.; Van Oosten, C. L.; Warner, M. *Phys. Rev. A* **2008**, *78*, 013823.
(12) Corbett, D.; Warner, M. *Phys. Rev. Lett.* **2007**, *99*, 174302.
(13) Serra, F.; Terentjev, E. M. *J. Chem. Phys.* **2008**, *128*, 224510.
(14) Warner, M.; Mahadevan, L. *Phys. Rev. Lett.* **2004**, *92*, 134302.
(15) Van Oosten, C. L.; Harris, K. D.; Bastiaansen, C. W. M.; Broer, D. J. *Eur. Phys. J. E* **2007**, *23*, 329–336.
(16) Cviklinski, J.; Tajbakhsh, A. R.; Terentjev, E. M. *Eur. Phys. J. E* **2002**, *9*, 427–434.
(17) Elias, A. L.; Harris, K. D.; Bastiaansen, C. W. M.; Broer, D. J.; Brett, M. J. *J. Mater. Chem.* **2006**, *16*, 2903–2912.
(18) Broer, D. J.; Mol, G. N.; Van Haaren, J. A. M. M.; Lub, J. *Adv. Mater.* **1999**, *11*, 573–578.
(19) *Polymer Handbook*, 3rd ed.; Brandrup, J., Immergut, E. H., Eds.; Wiley: London, 1989.
(20) *Copolymerization*; Ham, G. E., Ed.; Wiley: New York, 1964.
(21) Lin-Vien, D.; Colthup, N. B.; Fateley, W. G.; Grasselli, J. G. *The Handbook of Infrared and Raman Characteristic Frequencies of Organic Molecules*; Academic Press: San Diego, 1991.
(22) White, T. J.; Tabiryan, N. V.; Serak, S. V.; Hrozhyk, U. A.; Tondiglia, V. P.; Koerner, H.; Vaia, R. A.; Bunning, T. G. *Soft Matter* **_2008**, *4*, 1796–1798.

MA801802D